WAVE DAMPING AND PERMEABILITY SCALING IN RUBBLE MOUND BREAKWATERS

G. WOLTERS[1], M.R.A. VAN GENT[2], B. HOFLAND[3] & P. WELLENS[4]

[1] Deltares, Delft, The Netherlands, Guido.Wolters@deltares.nl

[2] Deltares, Delft, The Netherlands, Marcel.vanGent@deltares.nl

[3] Deltares, Delft, The Netherlands, Bas.Hofland@deltares.nl

[4] Deltares, Delft, The Netherlands, Peter.Wellens@deltares.nl

Abstract

Proper modelling of core material is essential in hydraulic model testing of rubble mound breakwaters, since it can significantly affect the wave damping process, and thus the amount of wave transmission and the stability of armour layers. In this study the wave damping process within 4 breakwaters was investigated at varying scales. Based on the results a simple scaling rule for the physical modelling of porous flow (permeability) is proposed.

Keywords: Rubble mound breakwater; Permeability scaling; Porous flow; Wave damping

1. Introduction

In order to assess the wave damping process in rubble mound breakwaters an experimental model investigation was carried out in the Scheldt Flume of Deltares. Four simplified breakwaters, with scaling relationships of 1:1, 2:1, 2.5:1 and 3:1 were tested and the pressure and water level distributions in the breakwater core were recorded. Furthermore, insight was sought into the scaling issues concerning the physical modelling of porous flow at small scale. The focus of the study was on wave transmission; effects of breakwater permeability on e.g. armour stability and wave overtopping were not investigated.

2. Damping of pressures inside the breakwater core

Data on wave damping within rubble mound breakwaters, especially for similar geometries but varying scales, is scarce. Pressure distributions within rubble mound breakwaters are presented e.g. by Bürger *et al.* (1988), Oumeraci & Partenscky (1990), Muttray & Oumeraci (2005), Troch *et al.* (1996) and Vanneste & Troch (2010). Based on the results of Bürger *et al.* (1988) and Troch *et al.* (1996), Burcharth *et al.* (1999) developed a hydraulic scaling model for the core material diameter in physical model tests. However, in their method and similar methods the damping of the wave inside the breakwater core is based on an empirical damping coefficient, which makes it difficult to assess the validity of the individual damping parameters. In the following a theoretical approach is introduced to derive the relevant damping parameters.

An estimate of the damping coefficient can be obtained using an exact solution for the linearized shallow-water equations inside a permeable structure. Here it is derived for one spatial dimension under the assumption of zero-mean flow:

$$\frac{\partial \zeta}{\partial t} + h\frac{\partial u}{\partial x} = 0 \quad \text{and} \quad \frac{\partial u}{\partial t} + g\frac{\partial \zeta}{\partial x} = -\hat{a}u \qquad [1+2]$$

In the continuity equation [1] and the momentum equation [2] ζ is the surface elevation with respect to MSL, h is the water depth, u is the depth-averaged velocity and g is the acceleration of gravity. Because of the linearization, the flow through the permeable structure is necessarily laminar. As a result, the resistance force inside the structure can be modeled with a Darcy coefficient times the velocity: $\hat{a}u$ (where $\hat{a} = g \cdot n_f \cdot a_{Forchheimer}$, $a_{Forchheimer}$ is the friction coefficient in the Forchheimer equation and n_f is the core porosity).

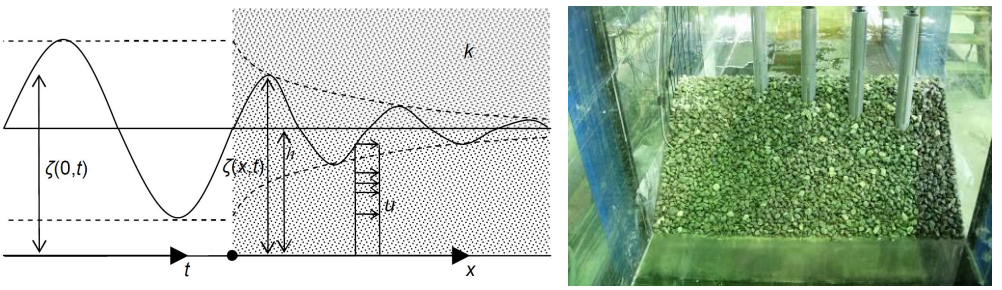

Figure 1. Illustration of the wave damping process within the breakwater core (left), set-up in Scheldt Flume (right).

Continuity equation [1] and momentum equation [2] can be combined into one equation for the depth-averaged velocity by taking the spatial derivative of the continuity equation and the time derivative of the momentum equation and eliminating the derivatives of the surface elevation ζ to obtain

$$\frac{\partial^2 u}{\partial t^2} - gh\frac{\partial^2 u}{\partial x^2} = -\hat{a}\frac{\partial u}{\partial t} \quad \text{with solutions of the form} \quad u = u_a e^{-\delta x} e^{i(kx-\omega t)} \qquad [3+4]$$

In Equation [4], ω is the radial frequency ($\omega = 2\pi / T$), k is the wave number ($k = 2\pi / L$) and δ is the rate of decay. The unknown coefficients that need to be resolved are k and δ. By expressing these coefficients in terms of the frequency a so-called dispersion relation can be derived. By taking the first- and second-order derivatives of u in Equation [4] with respect to space and time and substituting them into the Partial Differential Equation (PDE) for u in [3], the PDE becomes:

$$-\omega^2 u - gh\left(\delta^2 - k^2 - 2\delta i k\right)u = \hat{a} i \omega u \qquad [5]$$

From Equation [5], two equations may be derived: one equation for the imaginary part of [5] and one for the real part of [5]. From the imaginary part an expression for δ and from the real part a dispersion relation was found:

$$+2gh\delta ik = \hat{a} i\omega \;\Rightarrow\; \delta = \frac{\hat{a}\omega}{2ghk} \quad \text{and} \quad -\omega^2 - gh\left(\delta^2 - k^2\right) = 0 \qquad [6+7]$$

Now, by substituting the expression for δ [6] into the dispersion relation [7] and solving for the wave number k (neglecting imaginary expressions for the wave number) and the wave length in the core L_{core} (from here on only wave modes propagating in positive direction are considered):

$$k = \pm\sqrt{\frac{\omega^2 + \sqrt{\omega^4 + \left(\hat{a}\omega\right)^2}}{2gh}} \quad \text{and} \quad L_{core} = \frac{2\pi}{k} = 2\pi\sqrt{\frac{2gh}{\omega^2 + \sqrt{\omega^4 + \left(\hat{a}\omega\right)^2}}} \qquad [8+9]$$

The damping coefficient δ for the damped wave within the permeable medium [6] becomes:

$$\delta = \frac{\hat{a}\omega}{\sqrt{2gh}\sqrt{\omega^2 + \sqrt{\omega^4 + \left(\hat{a}\omega\right)^2}}} = \frac{\hat{a}\omega}{\sqrt{2gh}\cdot A(\omega)} \qquad [10]$$

It can be shown that the damping coefficient is the same for surface elevation, (depth-averaged) velocity and pressures within the permeable structure. The damping coefficient increases with increasing wave length, decreasing wave period, decreasing water depth, lower porosity and smaller material diameter (D_{n50}). However, due to the mentioned restrictions, the employed theory can cause problems with (very) short waves. The damping factor in Equation [10] is different from the empirically derived relationships from e.g. Burcharth *et al.* (1999) or Vanneste & Troch (2012). Note that no dependency on either $1/H_s$ or $1/b$ (b = core width) was found for the present investigation (e.g. Burcharth *et al.*, 1999); a dependency on the wave period was however found (see also [10]). The influence of the porosity and the core material parameters is included via $\hat{a}$ and is considered to be most relevant for a correct description of the damping process. A possible effect of b could not be verified conclusively, due to the almost complete wave damping within the structure. Included in Vanneste & Troch (2012) is also a dependence on the vertical position (z). This dependence, not included in the present theoretical approach, was not investigated in the present study and could thus not be verified.

3. Model set-up

The 2D physical model tests were carried out in the Scheldt Flume of Deltares. This wave flume has a length of 110 m, a width of 1 m and a height of 1.2 m. The wave generator is equipped with active reflection compensation (ARC) system to minimise reflections off the wave board. The test programme included four breakwater configurations. The geometry of the tested breakwater structures was the same for all configurations, only the geometric scale changed according to the scaling relationship of 1:1, 2:1, 2.5:1 and 3:1, see Table 1. The breakwaters consisted of a rock armour layer (rock armour thickness $t_a = 2D_{50,\ armour}$) and a rock core (no filter layer was used). The same $D_{n50,\ core}/D_{n50,\ Armour}$ was used for all test configurations. Front and rear slope had an inclination of 1:1.5. The set-up was based on a no-overtopping criterion with an upper core level at least 1 H_s above the employed SWL. This resulted in structure heights of 0.31m (Scale 1:1), 0.62m (Scale 2:1), 0.775m (Scale 2.5:1) and 0.93m (Scale 3:1), with crest freeboards of R_c = 0.11m - 0.33m. A horizontal foreshore was considered.

Before testing the porosity of the core material (respectively armour & core) was measured. The measured porosities were compared with the predicted values based on the grading curves (see CUR, 2007). The results show a good similarity between predicted and measured total porosities, all are approximately n_f = 0.44. This is also valid if the porosities of core and the total of armour and core are compared. The additional armour does not change the porosity of the overall structure significantly.

Table 1. Tested structure scales (h = water depth, h_s = structure height, B = crest width).

SCALE	h	h_s	B	$D_{n50,C}$	$D_{n50,A}$	$D_{85,C}$ /$D_{15,C}$	$D_{85,A}$ /$D_{15,A}$	SLOPE
	[m]	[m]	[m]	[mm]	[mm]	[-]	[-]	[-]
1:1	0.2	0.31	0.118	5	12	1.5	1.3	1:1.5
2:1	0.4	0.62	0.236	11	25	1.5	1.3	1:1.5
2.5:1	0.5	0.775	0.296	13	32	1.5	1.3	1:1.5
3:1	0.6	0.93	0.335	15	37	1.5	1.3	1:1.5

Measurements of the incident and transmitted wave heights were performed using 3 wave gauges positioned at the structure toe and behind the structure, the surface elevation within the structure core (using 5 wave gauges) and pressure measurements within the breakwater core. The pressure transducers were mainly located around the water line. 12 pressure sensors were installed, see Figure 2. From the adjacent pressure sensor positions the hydraulic gradients were determined.

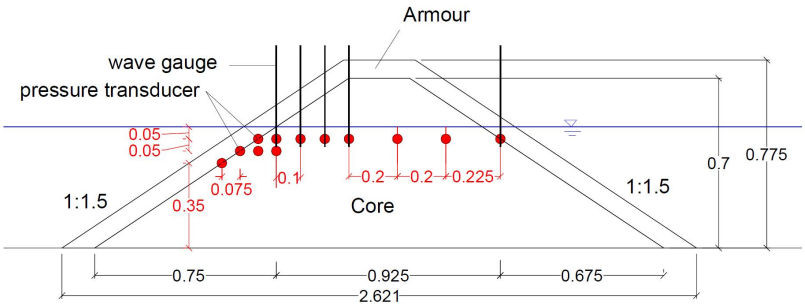

Figure 2. Set-up for scale 2.5:1 (Structure 4), in [m].

A fixed wave steepness of s_{op} = 0.02/0.03 was used with incident wave heights (H_{m0}, H) between 0.02-0.1m. The test durations consisted of 200 regular waves & 1000 irregular waves (JONSWAP, peak enhancement factor γ = 3.3). 4 test series were conducted with 12-16 tests each, that is 56 tests in total. All tests were conducted with a stable structure, i.e. no rock movement.

4. Test results

4.1 Flow characterisation

Based on Izbash & Khaldre (1970) the flow in the breakwater core can be characterized as laminar to transitional flow for all breakwater models. The laminar term (of the Forchheimer equation) is dominant for the smallest model, whereas laminar and turbulent terms are about equal for the 2:1 and 2.5:1 scale models and the quadratic term is dominant for the 3:1 model. For core material around D_{n50} = 5mm the flow is thus to be characterised as laminar and for larger material diameters as transitional. Fully turbulent flow could not be achieved in the breakwater core for all models. The damping coefficient (Equation 10, based on a laminar flow regime) is thus only an approximation and strictly valid only for hydraulic models of small scale. The comparison with the available large scale applications (Bürger *et al.*, 1988 and Troch *et al.*, 1996) will however show that a scale corrected damping term [15] appears to be

sufficient to accurately describe the damping behaviour within the breakwater core for those cases as well (note that even at large scale fully turbulent conditions are rarely found in the core).

4.2 Pressures, hydraulic gradients and velocities

The measured surface elevations and pressure amplitudes in the breakwater core for the various structure scales follow an exponential trend and show similar damping behavior (for both regular and irregular waves). The largest scatter in results is found for the smallest structure (Structure 1). The maximum pressure and surface elevation within the breakwater core (generally measured at the interface of armour layer and core) were found to be directly related to the incident wave height:

$$p_{0,2\%,IRR} = 0.72 \cdot \rho g H_{m0} \quad \text{and} \quad p_{0,2\%,REG} = 0.48 \cdot \rho g H \qquad [11]$$

$$\eta_{0,2\%,IRR} = 0.98 \cdot H_{m0} \quad \text{and} \quad \eta_{0,2\%,REG} = 0.74 \cdot H \qquad [12]$$

where $p_{0,2\%}$ is the 2% exceedance pressure measured at the interface of armour layer and core. Expressions [11] and [12] are strictly applicable only for the tested structure with an armour layer thickness of $2D_{50}$ and no filter layer. Note however that the magnitude is similar to the expressions found by Burcharth *et al.* (1999), i.e. $p_{max} = 0.5\ \rho g H_s$, and Vanneste & Troch (2010, 2012), i.e. $p_{max} = 0.6\ \rho g H_{m0} - 1.4\ \rho g H_{m0}$ (with a mean around $p_{max} = 1.0\ \rho g H_{m0}$), which have been derived for a structure with concrete armour and filter layer. Note also that the measured pressures for the regular wave tests were significantly lower than for the irregular tests.

A comparison of the predicted damping coefficient [10] with the measured damping coefficient (determined from Equation [16]) shows some scale related deviations. This is probably due to the fact that the applied shallow-water theory is not able to predict the damping behaviour correctly for very short waves and due to the variations in flow regime at various structure scales which are not sufficiently represented. A scale dependent correction factor c_s was therefore introduced, which depends on the core material diameter (for both pressures & surface elevations and irregular & regular tests the same factor c_s can be used):

$$\delta_{pred} = c_s \cdot \delta_{theory} \quad \text{with} \quad c_s = 278 \cdot D_{n50} - 0.7 \quad \text{and} \qquad [13]$$

$$c_{s,95\%} = 312 \cdot D_{n50} - 0.7 \quad \text{and} \quad c_{s,5\%} = 220 \cdot D_{n50} - 0.5$$

Alternatively c_s can be described using the Darcy coefficient $\hat{a}$ (which also includes the influence of the porosity n_f):

$$c_s = 11.2 \cdot \hat{a}^{-1/2} - 0.7 \quad \text{with} \qquad [14]$$

$$c_{s,95\%} = 12.6 \cdot \hat{a}^{-1/2} - 0.7 \quad \text{and} \quad c_{s,5\%} = 8.9 \cdot \hat{a}^{-1/2} - 0.5$$

With these corrections a good approximation of the measured damping coefficient is possible, see Figure 3 (left). The found relationship also seems to hold so far for large scale factors (see subsequent section), although additional verification is recommended. Note that the damping coefficients (plotted for all tested structure scales) of Le Méhauté (1957), Burcharth *et al.* (1999) and Vanneste & Troch (2012), see Figure 3 (right), show significantly more scatter and are not able to reproduce the damping correctly.

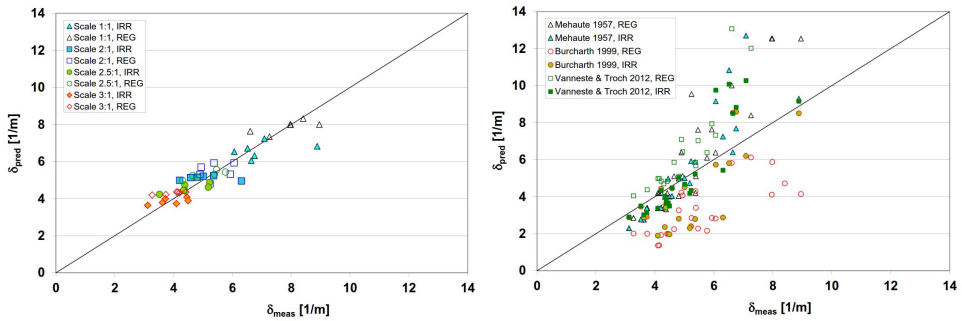

Figure 3. Predicted vs. measured damping factors (corrected with factor c_s); Left: new method, Right: comparison with methods of Le Méhauté (1957), Burcharth *et al.* (1999) and Vanneste & Troch (2012).

Based on the (scaled) damping coefficients of the pressure distribution, predictions can now be made of the hydraulic gradients within the breakwater core [15]. The prediction procedure for the hydraulic gradient within the breakwater core is based on the following approach:

$$I_{x,2\%} = \frac{1}{\rho g}\frac{\partial p}{\partial x} = -\frac{p_{0,2\%}}{\rho g}\cdot\delta\cdot e^{-\delta x} \qquad \text{with:} \qquad [15]$$

$$p_{2\%} = p_{0,2\%}\cdot e^{-\delta x} \quad (\text{resp.} \quad p_{2\%} = p_{0,2\%}\cdot e^{-\delta x}\cdot\cos(kx-\omega t)) \qquad [16]$$

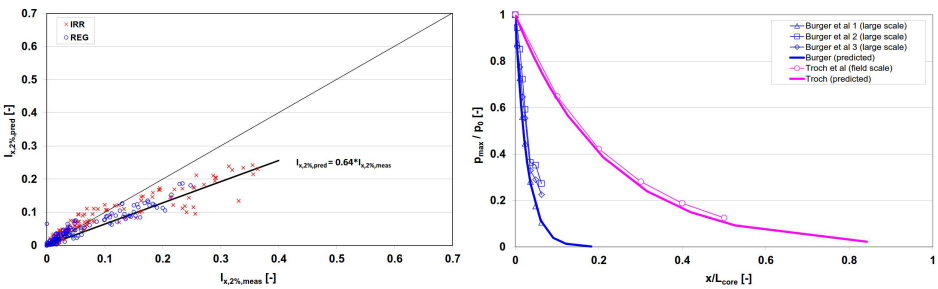

Figure 4. Left: Predicted vs. measured max. hydraulic gradient within core; Right: Predicted pressure distribution for large scale measurements of Bürger *et al.* (1988) and Troch *et al.* (1996).

As Figure 4 shows, the predictions consistently underestimate the measured hydraulic gradients (by 36%). However, a roughly linear trend was identified between predicted and measured values. This trend was consistent for all tested breakwater scales. Based on the observed trend, the following expression for the hydraulic gradient is proposed:

$$I_{x,2\%,pred,corr} = 0.64\cdot I_{x,2\%,pred} = -0.64\cdot\frac{p_{0,2\%}}{\rho g}\cdot(c_s\cdot\delta)\cdot e^{-(c_s\cdot\delta)x} \qquad [17]$$

The largest variations are found for small hydraulic gradients. From the (corrected) $I_{x,2\%}$ prediction the maximum filter velocities in the core can be calculated using the Forchheimer equation. The resulting trend can be described using Equation [18]:

$$\frac{u_{f,2\%}}{u_c} = 0.074\cdot I_{x,2\%} + 0.001 \quad \text{with} \quad u_c = \sqrt{gh} \qquad [18]$$

Please note that actual filter velocity measurements were not conducted. A correct filter velocity measurement within the core is very difficult and would require a closed off filter section with in- and outflow control.

4.3 Comparison with large scale and Zeebrugge (field) results

The new damping coefficient has been compared with large scale data of pore pressures by Bürger *et al.* (1988) and field scale data at Zeebrugge breakwater (Troch *et al.*, 1996). In Figure 4 (right) the found damping of the pore pressures is compared to the predicted damping using the new damping coefficient (Equation [13]). The figure shows that, as determined within this study, the damping increases with structure scale ($\delta_{pred} = c_s \cdot \delta$, Equation [13]). Based on the determined scaling relationships of $N_L = 6$ and $N_L = 60$ the new damping coefficient was calculated and from that the pressure distribution within the core. As can be seen from Figure 4, the estimation of the damping for the large scale tests of Bürger *et al.* (1988) and the field scale tests of Troch *et al.* (1996), using the new procedure, is good.

4.4 Conclusions

The tests showed that the proposed analytical solution of the shallow-water equations within a permeable structure is by itself not able to accurately resolve the damping behaviour within the breakwater core (pressures and surface elevations), because of the variations in flow regime at various structure scales (laminar, transient, turbulent regime) and the restrictions of the analytical model itself (e.g. inaccurate reproduction of short period waves). However, by applying scale-dependent correction factors in the description of the damping coefficient and the hydraulic gradient, an adequate reproduction of the test results could be achieved. A more sophisticated analytical model (for the transient flow regime and intermediate water depths) is not available. If more accurate estimates of damping behaviour are required, numerical model computations with models such as COMFLOW (Wellens *et al.*, 2010) or OpenFOAM (Jensen *et al.*, 2014) can be performed. Furthermore, additional large scale tests for the turbulent flow regime are strongly recommended (these would give additional information on scaling issues, since the b-term in the Forchheimer equation can usually be neglected at model scale, however generally not at field scale).

5. Scaling of core material in rubble mound breakwaters

5.1 Proposed scaling procedure

To decrease possible scale effects in physical modelling, core and filter materials are often scaled based on permeability. The scaling of permeability is achieved by equating the hydraulic gradient in prototype and model. This is usually implemented by equating the Forchheimer resistance for porous flow of the materials. The Forchheimer equation is:

$$i = a \cdot u_f + b \cdot u_f^2 \qquad [19]$$

where i is the hydraulic gradient (-), u_f the depth-averaged filter velocity (m/s), and a (s/m) and b (s^2/m^2) friction coefficients based on Van Gent (1995-a,b). The latter also include non-steady flow (cyclic flow) effects). Note that, if for example the laminar term is negligible (for sufficiently large core materials) at prototype scale, a simplified relationship will result.

Similarly, dependent on the flow regime, the turbulent term can be negligible at model scale. By applying Equation [17] for *i* the following relationship can be derived, where the indice m refers to model and p to prototype scale:

$$\frac{p_{0,2\%,p}}{\rho g}\cdot\left(c_{s,p}\cdot\delta_p\right)\cdot e^{-(c_{s,p}\cdot\delta_p)x_p}=\frac{p_{0,2\%,m}}{\rho g}\cdot\left(c_{s,m}\cdot\delta_m\right)\cdot e^{-(c_{s,m}\cdot\delta_m)x_m} \qquad [20]$$

This equation can only be solved numerically. However, by substituting Equations [11], [10], [13], $\hat{a} = g\cdot n_f \cdot a$, the (Froude) scaling factor N_L and using the assumption of $n_{f,p} = n_{f,m}$ and $x = 0$ a simplified equation can be derived:

$$D_{n50,m,corr}=N_L^{-2}\left(\frac{A(\omega_m)}{A(\omega_p)}\right)\left(D_{n50,p}-\frac{0.7}{278}\right)+\frac{0.7}{278} \quad \text{with} \quad A(\omega)=\sqrt{\omega^2+\sqrt{\omega^4+\left(\hat{a}\omega\right)^2}} \qquad [21+22]$$

where $\omega_m = \omega_p\cdot\sqrt{N_L}$. By assuming that $x = 0$ (and $n_{f,p} = n_{f,m}$), Equation [21] is strictly valid only for the front of the structure core ($D_{n50,m,corr}$ is expected to vary within the core. To achieve an averaged diameter over the entire core width Equation 20 needs to be solved numerically for various values of *x*). However, the simplified approach, Equation [21], is used here since it allows a quick calculation of the core diameter (and appears sufficiently accurate in the investigated test range, see subsequent paragraphs). By iteration (using the initially assumed value of $D_{n50,m} = D_{n50,p} / N_L$ for âm) the new core material diameter in the model can now be calculated from Equation 21 and from this the enlargement factor in relation to Froude scale. The resulting enlargement factor is displayed in Figure 5 (for 2mm < $D_{n50,core,Froude}$ < 9mm). For $D_{n50,\ Froude,\ model}$ > ~7mm (depending on c_s range: 4-9mm) the following relationships holds for the enlargement factor:

$$\frac{D_{n50,core,corr}}{D_{n50,core,Froude}}=1 \qquad [23]$$

For smaller diameters (< 2mm) the formula is not considered applicable due to strong viscous effects at that scale. Note that, based on the Izbash criterion, core diameters from 9mm are still in the transitional flow regime (and not yet fully turbulent). Equation [23] indicates that no enlargement of the core diameter is required for $D_{50,core,Froude}$ > 7mm (this corresponds to Re_f > 300, see next paragraph).

In Figure 5 (right) the enlargement factor is plotted against the Reynolds number in the filter Re_f, where $Re_f = u_f\ D_n\ /\ \nu$. It can be seen that for Re_f > 300 no enlargement of the core diameter is required. However, for smaller Reynolds numbers in the model the core diameter needs to be enlarged to ensure kinematic model similarity. The enlargement factor in relation to Froude scale can be described with (Figure 5, right):

$$\frac{D_{n50,core,corr}}{D_{n50,core,Froude}}=-0.455\cdot\log\left(\mathrm{Re}_f\right)+2.13 \qquad \text{for } \mathrm{Re}_f<300 \qquad [24]$$

$$\frac{D_{n50,core,corr}}{D_{n50,core,Froude}}=1 \qquad \text{for } \mathrm{Re}_f>300 \qquad [25]$$

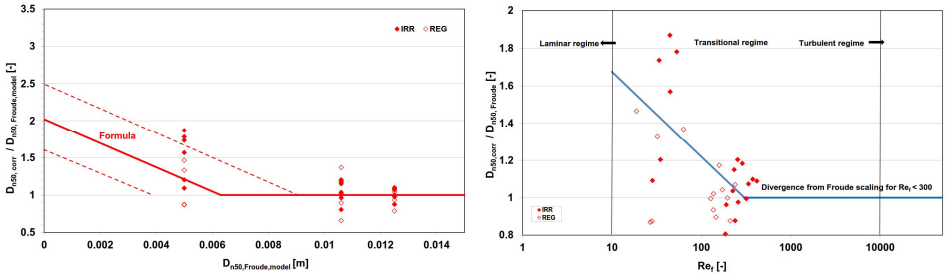

Figure 5. Enlargement factor for stone size; Left: Enlargement factor compared to Froude scaling; Right: Enlargement factor in dependence of Reynolds number Re_f; Straight red and blue line: Formula [21] and [24]; Dotted red line: Envelope for $c_{s,95\%}$, $c_{s,5\%}$ data; Red points: Measured data.

5.2 Comparison with measured data (based on u_f - scaling)

The results of Equation [21] (prediction of core material diameter) were checked based on the measurements within the core. The enlargement factor was thereby calculated for each test from the filter velocities (u_f is thereby iteratively computed from the measured hydraulic gradients, which in turn depend on the *KC* value in the core). The filter velocity is then scaled using Froude (very similar to the approach by Burcharth *et al.*, 1999) and the (corrected) core diameter determined using Forchheimer, see points in Figure 5 (left). This corrected core diameter is then compared to employed material diameter at reduced scale.

In contrast to Equation [21] (i.e. with x=0) the averaged filter velocities over the first half of the structure are used. Also, both Forchheimer coefficients (*a*,*b*) are used in contrast to the (simplified) theoretical approach which is based on *a* (and the empirically derived corrections using c_s). However, despite the involved simplifications in Equation 21, the approach provides similar results in the tested parameter range (see Figure 5, left).

6. Conclusions

The objective of this research was to assess the wave damping process in rubble mound breakwaters using physical model testing. Furthermore, insight was sought into the scaling issues concerning the physical modelling of porous flow (wave transmission) at small scale.

An experimental model investigation on the wave damping process in rubble mound breakwaters was carried out in the Scheldt Flume of Deltares. Four simplified breakwater structures, with scaling relationships of 1:1, 1:2, 1:2.5 and 1:3 were tested and the pressure and water level distributions in the breakwater core were recorded. The tests showed that the proposed analytical solution of the shallow-water equations within a permeable structure is by itself not able to accurately resolve the damping behaviour within the breakwater core, because of the variations in flow regime at various structure scales (laminar, transient, turbulent regime) and the restrictions of the analytical model itself (e.g. reproduction of short period waves). However, by applying a scale dependent correction factor (c_s) in the description of the damping coefficient and the hydraulic gradient, an adequate reproduction of the test results could be achieved. A more sophisticated analytical model (for the transient

flow regime and intermediate water depths) is not available. If more accurate estimates of damping behaviour are required, numerical model computations with models such as COMFLOW (Wellens *et al.*, 2010) or OpenFOAM (Jensen *et al.*, 2014) can be performed.

It is proposed to perform permeability scaling based on Equation [20]. Since this equation can only be solved iteratively, another (simplified) scaling rule is proposed for a first assessment of the proper core material diameter at model scale (Equation [21]). For smaller diameters (< 2mm), which are not recommended for application in small-scale physical model tests (see also Wolters *et al.*, 2009), the formulae are not considered applicable due to strong viscous effects at that scale.

It is recommended to perform additional large scale tests to verify the model for the turbulent flow regime.

References

Burcharth H.F., Liu Z. and Troch P., 1999. Scaling of core material in rubble mound breakwater model tests, *Proc. COPEDEC V conference*, *Cape Town SA*, pp. 1518-1528.

Bürger W., Oumeraci H., Partenscky H.W., 1988. Geohydraulic investigations of rubble mound breakwaters, *Proc. Int. Conf. on Coastal Engineering*, ASCE.

CIRIA, CUR, CETMEF, 2007, The Rock Manual. The use of rock in hydraulic engineering, 2nd edition, C683, CIRIA, London.

Izbash S.V. and Khaldre Kh.Yu., 1970. Hydraulics of river channel closure, Butterworths, London.

Jensen, B., Jacobsen, N.G., Christensen, E.D., 2014. Investigations on the porous media equations and resistance coefficients for coastal structures, *Coastal Engrg*, 84, pp. 56-72.

Le Méhauté B., 1957. The perviousness of rock fill breakwaters to periodic gravity waves. *La Houille Blanche*, 6.

Muttray M., Oumeraci H., 2005, Theoretical and experimental study on wave damping inside a rubble mound breakwater, *Coastal Engrg*, 52, 8, 709-725.

Oumeraci H., Partenscky H.W., 1990, Wave-induced pore pressure in rubble mound breakwaters, In: ASCE (Ed.), *Proc. ICCE*, pp.1334-1347, Delft, The Netherlands.

Troch P., De Somer M., De Rouck J., Van Damme L., Vermeir D., Martens J.-P., Van Hove C., 1996. Full scale measurements of wave attenuation inside a rubble mound breakwater, *Proc. ICCE 1996*.

Vanneste D. and Troch P., 2010. Experimental research on pore pressure attenuation in rubble-mound breakwaters, *Proc. ICCE 2010*.

Vanneste D. and Troch P., 2012. An improved calculation model for the wave-induced pore pressure distribution in a rubble-mound breakwater core, *Coastal Engineering*, 66, 8-23.

Van Gent M.R.A., 1995-a. Wave interaction with permeable coastal structures, Ph.D.-thesis, Delft University of Technology, Delft University Press, Delft. ISBN 90-407-1182-8.

Van Gent, M.R.A., 1995-b. Porous flow though rubble mound material, *J. of Waterway, Port, Coastal and Ocean Engineering*, Vol.121, no.3, pp.176-181, ASCE, New York.

Wellens, P.R., Borsboom, M.J.A. and Van Gent, M.R.A., 2010. 3D simulation of wave interaction with permeable structures, *Proc. ICCE 2010*, Shanghai.

Wolters, G., Van Gent, M.,. Allsop, W., Hamm, L., Mühlestein, D., 2009. HYDRALAB III: Guidelines for physical model testing of rubble mound breakwaters, *Proc. Coast, Marine Structures and Breakwaters 2009*, Edinburgh.